Meccanica (2006) 41: 341–349
DOI 10.1007/s11012-005-5902-8

A Molecular Dynamics Model for Single Adhesive Contact

F. A. GILABERT[1,*], A. M. KRIVTSOV[2] and A. CASTELLANOS[1]
[1]*Departamento de Electrónica y Electromagnetismo. Facultad de Física. University of Seville. Avenida Reina Mercedes s/n. 41012, Seville, Spain;* [2]*Department of Theoretical Mechanics, St. Petersburg State Technical University, Politechnicheskaya Street 29; 195251 St. Petersburg, Russia*

(Accepted: 9 September 2005)

Abstract. The normal adhesive contact between a pair of asperities is performed using molecular dynamics. To simplify the problem, the equivalent contact problem of sphere–plane interaction is solved. Displacements in the contact zone are very small compared to the asperity size, therefore, the computational model is focused on the neighborhood of the contact area. The adhesion between the asperity and the plane is calculated as a sum of interactions between atoms of the asperity and the plane. A computational experiment of pull-on and pull-off is carried out to study the influence of the adhesion on the formation of the contact forces and deformations. The numerical results are compared with theoretical predictions.

Key words: Computer modelling, Fine particles, Contact mechanics, Mechanical properties, Adhesion, Plasticity.

1. Introduction

The adhesive forces between fine particles play an important role in the mechanical behavior of cohesive powders. The fine granular materials with the constituent particle size in the range of 1–100 μm have a decisive importance in many industrial processes such as flow, compression, aggregation, dispersion, mixing, etc. Mechanical properties of the powder particles and the nature of the contacts between them are the keys to understand the mechanical behavior of fine cohesive powders. However these properties are not well known. Many factors such as geometry and size-distribution of particles, effects of the boundaries, and influence of external forces contribute to rise the complexity of the problem. The first stage to study these systems is to understand on the one hand the physics of a single contact and on the other hand the dynamics of a multi-contact system that implements features of the single contact. In this work, we will focus our attention on how a single adhesive contact can be modelled using direct numerical simulations. Different theories have been developed to understand a single normal elastic adhesive contact between spherical bodies [1–4]. In this work, a Molecular Dynamics technique is applied to study normal contacts between the powder particles, and the computational results are compared with the theoretical predictions of the Maugis–Pollock (MP) model [5],

*Author for correspondence: e-mail: gilav@us.es

which is based on the description of the plastic yield of the material in the contact zone.

2. Modelling of the Asperity Surface

For the powder particles the effective area of contact is given by the contact between small asperities [6, 7]. Therefore, to model the contacts between the powder particles a numerical model for the asperity is needed. Below we will describe the main features and parameters of this model. A representative value for the asperity radius is $R_{\text{asp}} \simeq 0.1\,\mu\text{m}$.

First, the appropriate computational model of the material is required possessing the same main mechanical properties (Young's modulus, Poisson's coefficient, and the ultimate strength) as the real material. As the material reference we have used polystyrene – a typical polymer material used in cohesive powder particles. Using molecular dynamics approach, this material can be represented as an amorphous ensemble of atoms interacting via an empirical potential. Parameters of this potential can be adjusted using uniaxial compression tests. In [8] it was shown that using the Lennard–Jones potential

$$\Pi(r) = D\left[\left(\frac{a}{r}\right)^{12} - 2\left(\frac{a}{r}\right)^{6}\right] \tag{1}$$

with the values of parameters listed in Table 1 gives a computer material with the mechanical properties close to polystyrene (see Table 2). We considered $T = 10^{-3} D/K_B \simeq 0.3\,K$ (T is the temperature, D the bond energy and K_B the Boltzmann's constant). Using this condition of low temperature, the computational tests of compression/tension provide the closest values of the theoretical elastic modulii (where temperature is not taken into account). Another consideration to use a low T is that actually we do not want include thermal effects because they can hide the purely mechanical ones (for example: a dilatation decreases the Young's modulus). In real pull-on/pull-off experiments with micron-sized particles the temperature has not any influence, because thermal effects are negligible in quasi-static contact interaction. Second, a sphere formed from the computer material is prepared. The radius of the sphere is equal to the average radius of asperity. Since the contact zone is much smaller than the size of the asperity, only a section of the prepared sphere was used in the computer experiments (see Figure 1). To simplify the computer experiment, the equivalent contact problem of sphere–plane interaction has been consid-

Table 1. Microscopical parameters of the computer material

Parameter	Symbol	Value	Unit
Equilibrium distance	a	$4 \cdot 10^{-10}$	m
Bond energy	D	$3.81 \cdot 10^{-21}$	J
Bond strength	$f_{\max}$	$2.56 \cdot 10^{-11}$	N
Bond stiffness	C	1.72	N/m
Atom mass	m	$4.77 \cdot 10^{-26}$	kg

Table 2. Macroscopical parameters of the computer material compared with polystyrene

Parameter	Symbol	Computer material	Polystyrene	Unit
Young's modulus	E	3.6	3.0	GPa
Poisson's coefficient	ν	0.38	0.33	–
Ultimate strength	σ_u	80	90	MPa
Strength ratio	σ_u/E	2.2	3.0	%
Density	ρ	1065	1065	kg/m^3

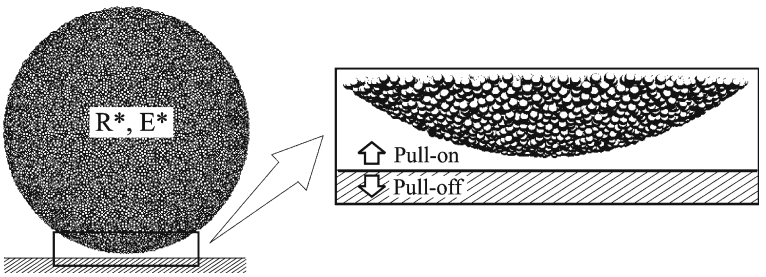

Figure 1. Scheme of the simulated setup. Up movement of the plane (rayed area) is a pull-on experiment, and down movement is a pull-off experiment.

ered. The plane is rigid and atoms belonging to the asperity are interacting with the plane to form the contact. In this paper, we will be considering the normal frictionless contacts only. Let us note that measuring the contact area at nanoscale is a challenging task since discreteness of the atomic structure brings an ambiguity to the area definition [9]. In the current paper to measure the contact area we assume that each atom contribute with an effective cross-section (typically πr_{eff}^2) that depends on the distance of interaction (not only the nearest–neighbors of the plane contribute to the macroscopical cross-section). To produce the necessary load during the computer experiments the plane is moved with a preset velocity. The atoms of the upper side of the asperity are clamped in their equilibrium positions. It is assumed that the asperity is thick enough so that the deformations initiated by the contact with the plane cannot affect much the clamped atoms. In the equivalent sphere–plane contact problem, the radius of the asperity and its elastic modulus are to be redefined as follows

$$\frac{1}{R^*} = \sum_i \frac{1}{R_i}, \qquad \frac{1}{E^*} = \sum_i \frac{1-\nu_i^2}{E_i}, \qquad i = 1, 2, \tag{2}$$

where R_i, E_i, and ν_i are the radius, Young's modulus, and Poisson's coefficient of sphere i, respectively [10].

To model the adhesive interaction between the asperity and the rigid plane, the analytical expression given by

$$U(z) = \int_V \Pi(r)\, \rho_n \, \mathrm{d}V = \frac{\pi \rho_n}{45} D^e a^3 \left[\left(\frac{a}{z}\right)^9 - 15 \left(\frac{a}{z}\right)^3 \right] \tag{3}$$

for the interaction energy between a single atom of the asperity and the plane has been used. In this expression, z is the atom-plane distance, ρ_n is the numerical density (number atoms per unit volume) in the plane, D^e is the bond energy between the separate atoms of the asperity and the plane. The integral is extended to the half-space volume occupied by the rigid plane. The relation between the bond energy between atoms D^e and inside the asperity D is given by $D^e \stackrel{\text{def}}{=} \xi D$, where ξ is a non-dimensional parameter that governs the adhesive strength. The work of adhesion w (the specific energy needed to separate two surfaces in contact) can be obtained as follows: (1) obtain the potential energy, $W(z)$, between two half-spaces integrating the expression 3 [11]; (2) calculate the equilibrium distance from $|W'(z)|_{z=z_{\text{eq}}} = 0$; and (3) substitute this equilibrium distance in $W(z)$. In this way, the work of adhesion w is

$$w = \sqrt[3]{\frac{15\pi^3}{512}}\,\rho_n\,\rho_n'\,D^e\,a^4, \tag{4}$$

where ρ_n and ρ_n' are the numerical density of atoms on both adhesive surfaces, respectively, separated by $z_{\text{eq}} = a/\sqrt[6]{15}$.

In the present work the polymer–polymer contacts ($\xi = 1$) will be of primary interest. The typical values of the work of adhesion w for polymers are within the interval 0.01–0.07 J/m^2. The calculation of w using the formula 4 and the parameters from Table 2 gives the value $w \simeq 0.04$ J/m^2, which is in a good agreement with the known experimental data [12].

3. Computer Pull-on and Pull-off Experiments

The force necessary to separate two powder particles can be obtained from so-called pull-on/pull-off experiments. The SFM[1] technology has made it possible to monitor the contact between very small particles [13, 14]. The relations between the interparticle force and displacement can be obtained from these experiment. In the presented work a computational setup similar to SFM technique has been prepared. The loading starts from a small distance between the asperity surface and the plane, and it continues until we get considerable values of the deformation. As it was mentioned above, during the computer experiments the controlling value is the displacement of the plane relatively to the clamped particles on the upper cross-section of the asperity. The relation between the pull-on force and the pull-off is recorded in the process of the experiment.

In Figure 2, a complete cycle of this computational experiment is shown. The key points of the process have been marked in this graph. The point (1) is the initial state of the specimen. When the asperity appears within the range of interaction with the plane, it suffers an extension due to the adhesive force. As we see in this graph, in point (2), the action of adhesive forces results in considerable deformation. To visualize this fact, we have intersected the stages of the specimen in points (1) and (2), where in the right-bottom picture in Figure 2c, the relative change of positions for some atoms can be seen. Most of the atoms were able to recover their initial position,

[1]Scanning Force Microscopy.

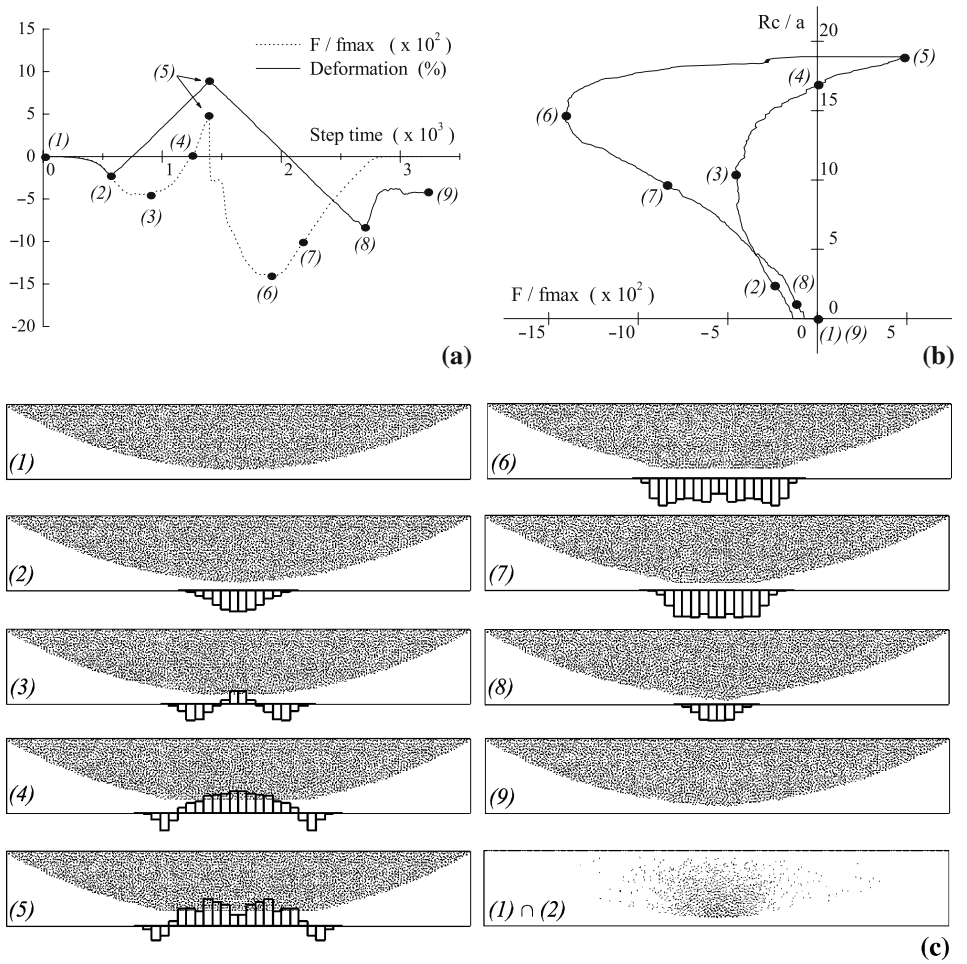

Figure 2. (a) – Deformation and force versus the number of computational steps. (b) – Radius of contact versus the force between the asperity and the plane. (c) – Pictures of the specimen that correspond to each point at graphs (a) and (b). The vertical bars are the distribution of the normal stress at the contact (upward direction is compressive stress, downward is tensile one). Let us note the tensile stress at the edges of the contact in points (3–5) caused by the attraction forces. The right-bottom picture shows the changes between the initial state, point (1), and the tensile deformation promoted by the adhesive force, point (2). In this last picture, the distribution of black points are relative internal displacements of atoms inside the material as a result of the adhesion. It can be noted that the larger displacements take place closer to the surface.

however, atoms close to the surface were permanently affected. In point (3), the maximal adhesive force is attained. At point (4), the total contact force is zero, therefore, repulsive and attractive forces are equilibrated. At point (5), the maximal compressive deformation is reached. This point corresponds with the pull-on force in this experiment. Note for both latter points the adhesive force acting on the edges of the contact. The next points correspond to the process of separation or pull-off action. Point (6) is the maximum force during the separation. This should be the force that one would have to exert on the grain to take it apart from the surface. Point (7) is an intermediate point while the asperity is removed and point (8) is when the separation

takes place. At both latter points one can see a weak neck formation. Point (9) is the final state after the computer experiment. It can be noted that finally the adhesion results in the enlargement of the apparent deformation of the surface. Let us note that the material has yielded plastically during the compression as well as during the separation. We have been able to see that during compression the material was deposited on edges, increasing more and more the effective radius of contact.

Some discussion about these results is pertinent. Let us note, that if the specimen deformation would have been purely elastic – first, the force in point (3) would correspond to the pull-off force predicted by DMT model [2] and – second, the maximum pull-off force in point (6) should be equal to the value obtained in the point (3). However, both values are different. According to the DMT model, the relation between the force required to separate two small hardly deformable spheres and the work of adhesion is

$$F_{\mathrm{DMT}} = -2\pi R^* w. \tag{5}$$

For the present material, this value is $F_{\mathrm{DMT}} = -12.2\,\mathrm{nN}$. The computed value was $F = -11.7\,\mathrm{nN}$. Therefore, an acceptable but partial agreement with this value of the force for the point (3) can be observed. Let us consider the Tabor's parameter [3]

$$\mu = \left(\frac{R^* w^2}{z_0^3 (E^*)^2} \right)^{1/3}, \tag{6}$$

which is the ratio between the amplitude of the elastic deformation when the contact is broken and the range of interaction of the adhesive forces. The quantity z_0 is the minimum possible distance between the adhesive surfaces. The computed value for the current simulations was $z_0 = 0.6498a$, which is very close to the theoretical value of $z_{\mathrm{eq}} = a/\sqrt[6]{15} \simeq 0.6368a$ used to derive the formula 4. Both distances have not to be equal, but they actually are very close. For this numerical experiment $\mu = 0.7$. In the literature it is accepted that the DMT model is applicable when $\mu < 0.1$. But when $\mu > 5$ the JKR model [1] is more appropriate. Therefore, this problem is just in the middle between these cases and it could explain the disagreement with the value in the force at the point (3). In addition, the value predicted by the adhesive elastic models differs from the maximum pull-off force computed for this specimen [point (6)]. It means that in this experiment the specimen does not behave elastically, and therefore, the plasticity should be taken in consideration.

Let us compare with the theoretical prediction of MP model [5] taking into account the plastic behavior. This theory is based on the assumption of elastic recovery of fully plastic contact. According to the MP model, the equilibrium force balance at the contact is given by the equation

$$F + 2\pi w R^* = \pi R_c^2 H, \tag{7}$$

where F is the external load, w the work of adhesion, R^* the reduced radius, R_c the radius of the area of contact, and H is the hardness of the material. The MP model assumes that the contact profile of pressure is Hertzian, but with the radius of curvature changed due to the plastic deformation. The new reduced radius of curvature is given by

$$F_{\text{Hertz}}(R^{*'}) = \pi R_c^2 H \quad \rightarrow \quad R^{*'} = \frac{R_c E^*}{\pi H}. \tag{8}$$

Maugis and Pollock also assume that the necessary force to separate two adhesive spheres after loading is given by JKR as follows

$$F_{\text{JKR}} = -\frac{3}{2}\pi R^{*'} w. \tag{9}$$

First we find the value of R_c from (7). Second, R_c is substituted in (8), and finally, the value $R^{*'}$ is inserted in (9). Then we obtain the relation between the pull-off force and the total load at the contact

$$F_{\text{pull-off}} = \frac{3}{2}\frac{w E^*}{\sqrt{\pi H^3}}\sqrt{F + 2\pi w R^*}. \tag{10}$$

In Figure 3, the theoretical prediction of the MP model is represented together with the numerical results obtained from the simulated performance. For the most values of the load a good agreement can be observed. Results from the computational model seem to differ for the largest values of the load. The possible explanation of this disagreement is that the plastic deformation, which takes place inside the computer material is larger than the one predicted by MP model. Probably, an unconfined plastic flow that provoke the deposition of material on the edges of the contact (as was commented on before) can be the reason of this disagreement. This plastic flow can increase the effective area of the contact, resulting in the increase of the pull-off force.

Finally we are going to calculate the mean stress due to the adhesion. The typical values of the adhesive force and the contact radius for this simulation are within the interval $|F_{\text{adh}}| = 10$–$70\,\text{nN}$ and $Rc = 10$–$80\,\text{Å}$, respectively. Let us chose the values corresponding to the beginning of the contact [point (3) in Figure 2]: $|F_{\text{adh}}| \simeq 12\,\text{nN}$ and $R_c \simeq 40\,\text{Å}$. The stress due to the adhesion is $|F_{\text{adh}}|/\pi R_c^2 = 239\,\text{MPa}$. This value clearly shows that the level of stress produced by the adhesion largely exceeds the resistance of the computer material making the plasticity unavoidable.

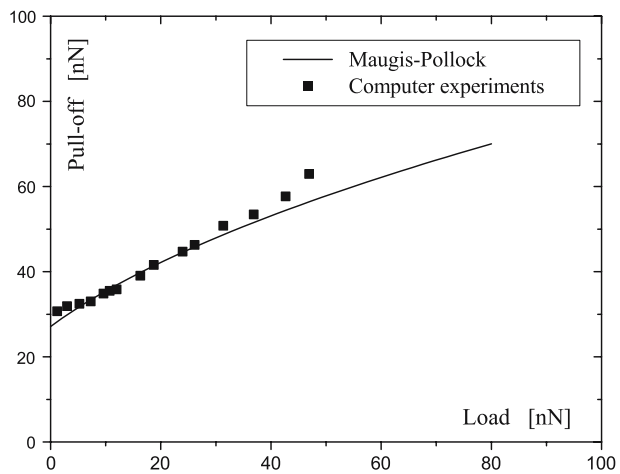

Figure 3. Comparison of the results of the MP theory and the pull-on/off computer experiments.

4. Conclusion

In the presented work a Molecular Dynamic simulations of the pull-on/off experiments for adhesive elastic–plastic contacts have been performed. A microscopical model of adhesion between elemental constituents (atoms) has been proposed. The contact between asperities has been simulated using the equivalent contact sphere–plane problem. This model simultaneously incorporates elasticity, plasticity, and adhesion, which is extremely difficult for theoretical considerations. The proposed model also takes into account the discreteness of the material surfaces at the nanolevel. These properties are usually abandoned by the theoretical or computational approaches, based on continuum mechanics. The stress–strain diagrams depend on the way one is determining the contact area, and this is the essential feature of the mechanical systems at nanolevel, which is usually lost in macroscopical considerations. Comparison of the obtained results with the theoretical predictions of Maugis–Pollock model showed a good agreement. Finally, Molecular Dynamics approach, showing good agreement with theoretical considerations of the normal contacts, can be a promising method to study complicated contact problems with adhesion, where the effects such as friction, oblique loading, rolling, or spinning lacks the theoretical understanding.

Acknowledgements

This research was supported by Spanish Government Agency Ministerio de Educación y Ciencia under Contract No. BFM2003-01739, Acción Integrada Hispano-Francesa No. HF2001-0127, NATO Collaborative Linkage Grant PST.CLG.976575, and RFBR grant No. 02-01-00514.

References

1. Johnson, K.L., Kendall, K. and Roberts, A. D., 'Surface energy and the contact of elastic solids', *Proc. R. Soc. Lond. A* **324** (1971) 301.
2. Derjaguin, B. V., Muller, V. M. and Toporov, Y. P., 'Effect of contact deformation on the adhesion of particles', *J. Colloid. Inter. Sci.* **53**(2) (1975) 314.
3. Tabor, D., 'Surface forces and surface interactions', *J. Colloid. Inter. Sci.* **58**(1) (1977) 2.
4. Greenwood, J.A. and Johnson K.L., 'An alternative to the Maugis model of adhesion between elastic spheres', *J. Phys. D: Appl. Phys.* **31** (1998) 3279.
5. Maugis, D. and Pollock, H.M., 'Surface forces, deformation and adherence at metal microcontacts', *Acta Metallurgica* **32** (1984) 1323.
6. Massimilla, L. and Donsi, G., 'Cohesive forces between partices of fluid-bed catalysts', *Powder Technol.* **15** (1976) 253.
7. Mason, T., Levine, A., Ertas, D. and Halsey, T.T.C., 'Critical angle of wet sandpiles', *Phys. Rev. E* **60** (2000) 5044.
8. Gilabert, F.A., Krivtsov, A.M. and Castellanos, A., 'Computer simulation of mechanical properties for powder particles using Molecular Dynamics' *Proceeding of XXX Summer School "Advanced Problems in Mechanics"*, pp. 230–239, 2002.
9. Krivtsov, A.M. and Morozov, N.F., 'Anomalies in mechanical characteristics of nanometer-size objects', *Doklady Phy*. **46**(11) (2001) 825.
10. Johnson, K.L., *Contact Mechanics*. Cambridge University Press, Cambridge, 1985.
11. Israelachvili, J.N., *Intermolecular and Surface Forces*. Academic Press, London 2nd ed., 1991.

12. Ross, S. and Morrison, I.D., *Colloidal Systems and Interfaces*. Willey-Interscience, New York, 1988.
13. Binnig, G., Quate, C.F. and Gerber, Ch., 'Atomic force microscope', *Phys. Rev. Lett.* **59**(9) (1986) 930.
14. Quintanilla, M.A.S., Castellanos, A. and Valverde, J.M., 'Correlation between bulk stresses and interparticle contact forces in fine powders', *Phys. Rev. E* **64**(3) (2001) 031301, 1–9.